Journal of the European Ceramic Society 21 (2001) 1027–1035

www.elsevier.com/locate/jeurceramsoc

Colloidal processing of Al_2O_3-based composites reinforced with TiN and TiC particulates, whiskers and nanoparticles

Eric Laarz [a], Mats Carlsson [b,*], Benoît Vivien [a], Mats Johnsson [b], Mats Nygren [b], Lennart Bergström [a]

[a] *Institute for Surface Chemistry, PO Box 5607, S-114 86 Stockholm, Sweden*
[b] *Department of Inorganic Chemistry, Stockholm University, S-106 91 Stockholm, Sweden*

Received 29 June 2000; received in revised form 13 October 2000; accepted 21 October 2000

Abstract

A colloidal processing route has been developed for the preparation of dense and homogeneous Al_2O_3–TiN/TiC composites. The dispersion and rheological properties of mixtures of TiN or TiC particulates and Al_2O_3 particles were investigated using electrokinetics and steady-shear rheology. We found that well-dispersed aqueous suspensions with low viscosity could be prepared by adding a poly(acrylic acid) dispersant and controlling pH in the alkaline range. This processing scheme was also suitable for preparation of whisker and nanoparticle composite suspensions. The alumina-based composite suspensions with a secondary-phase concentration of 25 vol.% were freeze-granulated and hot-pressed, and the resulting bodies were fully densified with well-dispersed secondary phases. Homogeneous Al_2O_3–TiN nanoparticle composites could only be prepared with additions of up to 5 vol.% nanoparticles; higher additions resulted in agglomeration and subsequent grain growth of the nanoparticles.

Keywords: Al_2O_3–TiC; Al_2O_3–TiN; Composites; Microstructure-final; Suspensions; TiC; TiN

1. Introduction

Mechanical properties of ceramic materials are strongly dependent on their microstructure. The fracture toughness, for instance, can be improved substantially by adding a secondary reinforcing phase to the matrix. It has been shown that the addition of a TiN or TiC phase to an alumina matrix increases hardness, fracture toughness and thermal shock resistance at temperatures up to 800°C.[1] In order to optimize the properties, the reinforcing particulate phase must be well dispersed in the matrix. Mixing, deagglomeration and dispersion of the reinforcing components are commonly performed in a liquid medium, preferably water. Additions of dispersing agents and/or manipulation of the solution properties, e.g. the pH value, are frequently used to optimize the suspension properties.

In this work, we have attempted to develop an aqueous colloidal processing route for preparating well-dispersed powder mixtures in the Al_2O_3–TiN/TiC systems, which upon densification would yield dense compacts with homogeneous microstructure. Based on thorough powder characterization and on the results of dispersion experiments, we have developed an optimized processing scheme and assessed its applicability to systems containing TiN and TiC with a wide range of morphologies. Thus, the preparation of composites containing micronsized TiN and TiC particles, nanosized TiN particles, and TiC and Ti(C,N) whiskers has been investigated. The results will be applied in a forthcoming investigation of the mechanical properties (e.g. thermal shock resistance) of Al_2O_3–TiN/TiC compacts. Experimentally, our study has included mainly electrokinetic and rheological characterization of aqueous composite suspensions and microstructure evaluation of sintered bodies by means of scanning electron microscopy.

2. Experimental

2.1. Powder characterization

The manufacturer specifications of the starting powders are given in Table 1. For simplification we will refer to the nano- and micronsized titanium nitride powders

* Corresponding author.
E-mail address: matsc@inorg.su.se (M. Carlsson).

0955-2219/01/$ - see front matter
PII: S0955-2219(00)00302-2

as TiN_{nano} and TiN, respectively. BET-surface area and particle-size distribution measurements of the as-received TiC, TiN and TiN_{nano} powders were obtained by means of BET nitrogen adsorption analysis (Flow Sorb II 2300, Micromeritics, USA) and X-ray gravitational sedimentation analysis (SediGraph 5100, Micromeritics Instrument Corporation, USA), respectively. Scanning electron microscopy, SEM (JEOL 880, Japan), and transmission electron microscopy, TEM (JEOL 2000FX, Japan), were employed to gain information on the particle morphology (Fig. 1). X-ray powder diffraction (XRD) patterns of the TiC and TiN powders were obtained using a Guinier-Hägg focusing camera with subtraction geometry. Cu-$K_{\alpha 1}$ radiation

Table 1
Manufacturer specifications showing particle size and chemical analysis for the different powders used

	TiC	TiN	TiN_{nano}	Al_2O_3
Manufacturer	H.C. Starck (Germany)	H.C. Starck (Germany)	H.C. Starck (Germany)	Sumitomo (Japan)
Powder Grade	STD 120	Grade C	nano TiN	AKP 30
Particle size (μm)	1.4	1.05	0.03 (BET equivalent spherical diameter)	0.3
N (wt.%)	0.15	20.8	21.9	–
C_{total} (wt.%)	19.5	0.05	0.009	–
C_{free} (wt.%)	0.4	–	–	–
$C_{combined}$ (wt.%)	19.1	–	–	–
O (wt.%)	0.6	1.2	0.5	–
Cl (wt.%)	–	-	3.7	–
Si (ppm)	60	50	< 50	< 40

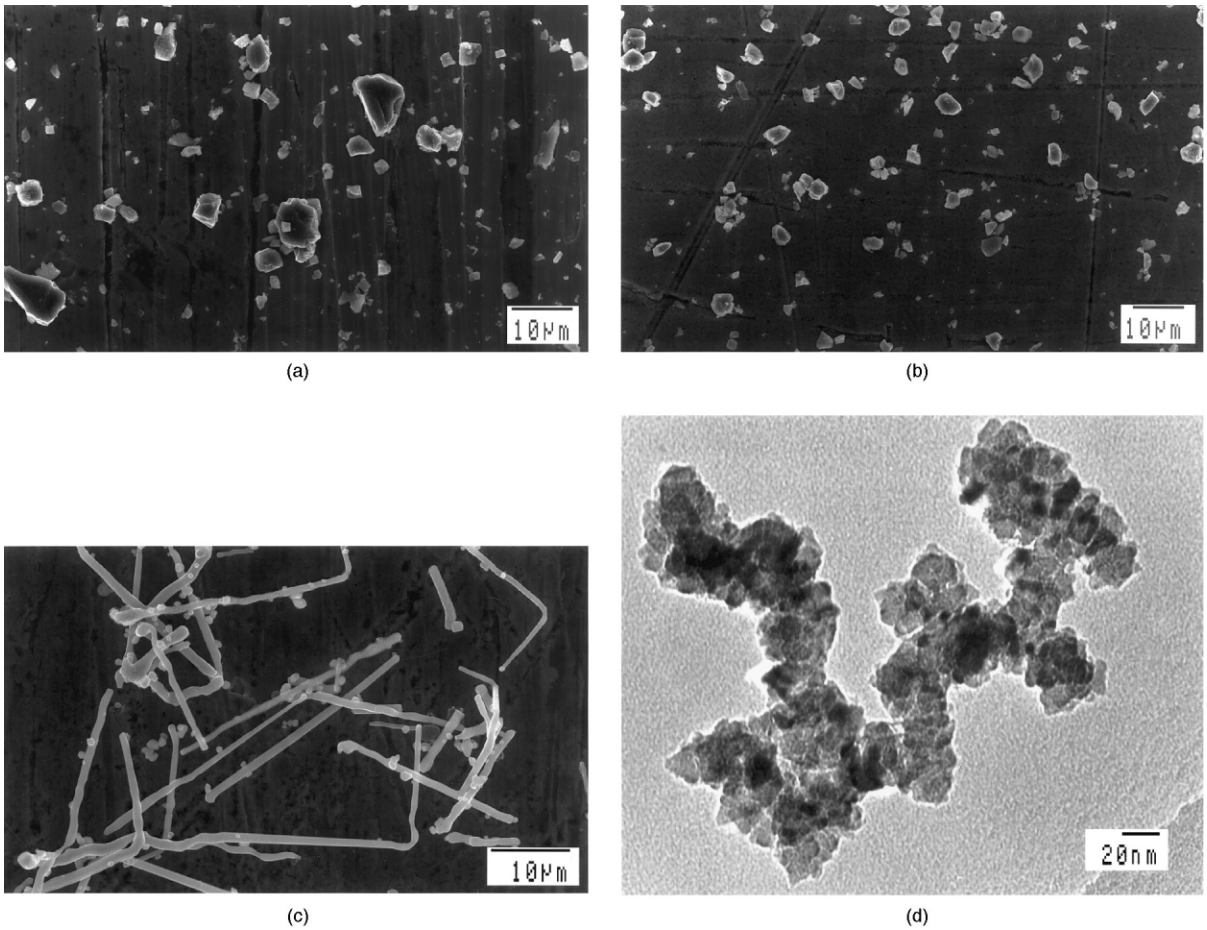

Fig. 1. Micrographs of as-received powder and whisker materials: (a) TiC; (b) TiN; (c) $Ti(C,N)_{whiskers;}$ (d) $TiN_{nano\ particles}$.

($\lambda = 1.54060$ Å) was used, and finely powdered silicon [$a = 5.430880(35)$ Å] was added as an internal standard. The recorded films were evaluated in an automatic film scanner,[2] and the unit cell dimensions were refined with the program PIRUM.[3] The XRD peaks were identified by matching them to ICDD data cards of TiC (ICDD card No.32-1383) $a = 4.3274$ Å, and TiN (ICDD card No. 38-1420) $a = 4.2417(1)$ Å. XPS analysis of the TiN and TiC particle surface composition was performed using a Mg–K_α X-ray source and a magnetic collimator lens (AXIS-HS, Kratos Analytical, UK). The powder solubility was assessed by determining the Ti concentration in solution after ageing in pH = 0.8, 6, 10 and 12 solutions for 1750 h. Ti was analyzed with a DCP (direct current plasma) emission spectrometer (Spectra-Span IIIB, SpectraMetrics Inc., USA). Microelectrophoresis (Zeta Sizer 2000, Malvern Instruments, UK) was used for electrokinetic characterization of TiN and TiC particles suspended in 0.01 M NaCl electrolyte. Zeta-potential measurements of concentrated (5 vol.%) alumina suspensions (0.01 M NaCl background electrolyte) were carried out with an AcoustoSizer™ instrument (Matec Applied Science, USA). We used analytical grade chemicals (Merck AG, Germany) for adjustment of ionic strength (NaCl) and pH (HCl and NaOH).

TiC whiskers and Ti(C,N) whiskers were synthesized at 1425 and 1250°C respectively via the carbothermal vapour–liquid–solid growth mechanism.[4,5] The whiskers have a length of about 10–30 μm and an aspect ratio of 15–50 (Fig. 1c). The TiN_{nano} powder is pyrogenic and was therefore suspended in a water–ethanol mixture (95/5 wt.%) in a glove box filled with nitrogen to promote a controlled surface oxidation.[6] After this treatment, the solvent was evaporated at 50°C.

2.2. Preparation and characterization of suspensions

Concentrated suspensions were prepared by mixing Al_2O_3 powder with deionized water until the required powder volume fraction was reached. The required amount of poly(acrylic acid) dispersant (Dispex A40, Allied Colloids, USA) had been dissolved in the deionized water prior to mixing. The anionic polyelectrolyte used (denoted as PAA) is an ammonium salt of poly(-acrylic acid) with a mean molecular weight of $M_w =$ 10 000 and a polydispersity of $M_w/M_n = 1.56$.[7] PAA concentrations are given in wt.% with respect to the alumina dry-powder weight. In a first milling step, alumina and PAA were mixed for 30 min at 400 rpm in a planetary ball mill (Pulverisette 6, Fritsch GmbH, Germany) equipped with a 250 ml SiAlON milling jar and SiAlON milling spheres (Ø = 10 mm). After this first step, the other solid phase (TiC, TiN, TiN_{nano} or whiskers) was added and the sample was milled for another 10 min. The obtained suspensions were rolled on a roll bench for 4 h in order to equilibrate. Afterwards, suspensions were sprayed through a nozzle into liquid nitrogen for granulation and were then freeze-dried. The obtained granules were sieved, and the $0.125 < d < 0.32$ mm fraction was used for the sintering experiments. Rheological evaluation was performed on suspensions that had been equilibrated by 4 h of magnetic stirring. All rheology experiments were carried out with a controlled-stress rheometer (UDS 200, Physica Messtechnik GmbH, Germany) equipped with a concentric cylinder measuring geometry.

2.3. Burnout and hot-pressing

The burnout of PAA was studied in a thermogravimeter, TG (TAG24, Setaram, France) in Ar–6% H_2 atmosphere. Prior to sintering, the organic content was burned out in a graphite furnace (Thermal Technology Inc., USA). Freeze-dried granules were poured directly into the die of a hot press (Thermal Technology Inc., USA), and the sample was subjected to 28 MPa at 1700°C for 1.5 h in flowing argon atmosphere. Densities of sintered bodies were measured according to Archimedes' principle. The expected densities of the sintered materials were calculated assuming no reactions to take place between the components and by using the following densities: $\rho_{A1203} = 3.965$ g cm^{-3}, $\rho_{TiN} = 5.22$ g cm^{-3}, $\rho_{TiC} = 4.930$ g cm^{-3}. The microstructure was evaluated with an SEM (880, JEOL, Japan). The composites containing TiN_{nano} were thermally etched at 1500°C for 15 min in flowing Ar in order to reveal their microstructure.

3. Results and discussion

3.1. Powder characterization

The TiC and TiN powders displayed similar particle morphology, particle size distribution, and surface area. Equiaxed grains with sharp edges were characteristic features of both the TiN and the TiC particle morphology (Fig. 1). The experimentally determined particle size distributions and specific surface areas are reported in Table 2. The TiC and TiN powders were characterised by XRD to be monophasic with a cell axis of $a =$ 4.32882(9) Å for TiC and $a = 4.23910(18)$ Å for TiN. In previous XRD studies of nano-sized TiN with much higher oxygen content (an order of magnitude higher than for the TiN_{nano} used in our study), traces of anatase and a substoichiometric TiO_{2-x} phase could be detected.[8,9] XPS analysis of the TiC and TiN powder surfaces indicated presence of an oxidized surface layer and a 20–25 at.% level of surface contamination by aliphatic carbon, which is substantially higher than the 3–10 at.% usually observed for high-purity ceramic powders.

The solubility of TiC and TiN powders in water is negligible (< 6 ppm Ti) over practically the entire pH range; only under very acidic conditions (pH = 0.8) significant concentrations of dissolved Ti (~100 ppm) could be observed. The surface oxides passivate the TiN and TiC materials, protecting them from further oxidation in aqueous environments.

3.2. Dispersion in aqueous medium

The oxidized TiC and TiN powders exhibited identical isoelectric points at $pH_{iep} \approx 4.3$ in NaCl electrolyte solutions (Fig. 2). The isoelectric point of TiC whiskers was determined to be $pH_{iep} \approx 4.3$ as well. In comparison, the isoelectric point of the α-alumina powder is much higher ($pH_{iep} \approx 9.2$). However, as shown in Fig. 2, upon addition of 0.5 wt.% PAA to the alumina suspension the pH_{iep} shifts to acidic values ($pH_{iep} \approx 3$) due to polyelectrolyte adsorption.[10–12] Measurements at various ionic strengths confirmed that NaCl acts as an indifferent electrolyte in all cases (not shown). The zeta-potential values for Al_2O_3 suspensions compare very well with previous results.[10–12] Previously reported pH_{iep}-values for TiN and TiC powders are somewhat less consistent with our results; different grades of TiN powders showed pH_{iep} in the range pH = 3–5,[8,9,13,14] and $pH_{iep} \approx 2$ has been found for TiC.[15] However, since non-oxide ceramic powders are thermodynamically unstable in air and water, these differences are not unexpected and can be attributed mainly to different degrees of surface oxidation. For example, it has been shown earlier that the synthesis route and post-synthesis treatment of Si_3N_4 powders strongly affect the surface oxygen content and the correlated area density of potential-determining surface groups.[16,17] Accordingly, increasing surface oxidation will shift the isoelectric point of the acidic TiN and TiC powders more and more towards the value for the less acidic oxide TiO_2 ($pH_{iep} \approx 6$).[18]

Table 2
Particle size distribution and specific surface area of the as-received TiC and TiN powders

	TiC	TiN	TiN_{nano}
Particle size distribution (μm)			
d_{16}	1.5	1.2	–
d_{50}	3.2	2.1	–
d_{84}	5.4	3.4	–
BET surface area ($m^2\ g^{-1}$)	2.7	3.1	44.9
BET equivalent spherical diameter (μm)	0.45	0.37	0.026

Based on our studies of the surface chemistry of TiN and TiC, we developed the processing scheme depicted in Fig. 3, which can be employed for preparation of Al_2O_3–TiN/TiC composite suspensions and sintered bodies. As shown in detail in previous work,[8–10] well-dispersed α-Al_2O_3 suspensions with an inherent suspension pH value of ≈9 are obtained by simply mixing deionized water, powder, and > 0.2 wt.% ammonium salt of PAA. According to our processing scheme, this is done in the first milling step and in the next milling step TiN or TiC is added. In this manner heterocoagulation is prevented, as can be seen from steady-shear measurements on suspensions with 20 vol.% solids loading (Fig. 4). Before and after adding TiN or TiC, the suspensions show almost no shear thinning, thus indicating a well-dispersed suspension. However, if addition of PAA is omitted, a flocculated, strongly shear-thinning suspension is obtained (Fig. 4). Clearly, the absence of flocculation is related to the electrostatic repulsion between alumina particles with adsorbed PAA layers

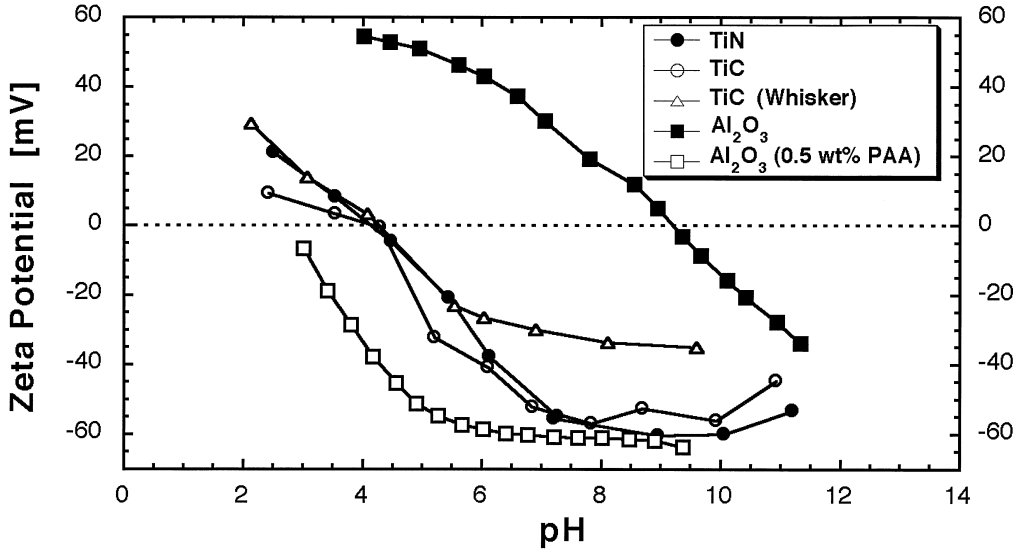

Fig. 2. Zeta potentials of the powders used in 0.01 M NaCl electrolyte solution.

and TiN or TiC particles which, according to Fig. 2, are also highly negatively charged at pH = 9.

Viscosity measurements on 20 vol.% TiC suspensions (Fig. 5) suggest that the negative surface charge is high enough at pH = 7.7 to prevent homocoagulation. At lower pH the surface charge is apparently too low, though, and flocculation takes place. In comparison, the pH of TiN samples must be increased to 10 to achieve a well-dispersed suspension with a Newtonian shear response (Fig. 5). Fig. 6 shows the flow curves of composite suspensions containing TiN_{nano}. Using nano-sized TiN up to 5 vol.% of the total solids loading does not change the flow behavior compared to suspensions containing 25 vol.% micron-sized TiN. A slight viscosity increase at 10 vol.% TiN_{nano} concentration is observable, and even higher concentrations lead to substantial shear-thinning (Fig. 6). This effect might be related to a crowding effect or an induced aggregation due to changes in suspension pH with addition of TiN_{nano}. The pH of an alumina suspension dispersed with 0.5 wt.% PAA decreases from 9.1 to 8.2 upon addition of 20 vol.% TiN_{nano} which can result in enhanced homocoagulation of the TiN particles (Fig. 5). Another factor contributing to the high viscosity might be the interaction between TiN_{nano} particles and PAA macromolecules. Previous results on the electrokinetics and rheology of TiN_{nano} particles dispersed with polyacrylic-type dispersants[8,9,14] imply that PAA can be adsorbed on titanium nitride. These studies suggested that adsorption occurs even at a pH where both particles and polymer carry negative charges. Hence, it is possible that in our system weak adsorption (i.e. adsorption below saturation level) of PAA on TiN_{nano} causes bridging flocculation at high TiN_{nano} particle concentrations and, thus, a higher suspension viscosity.

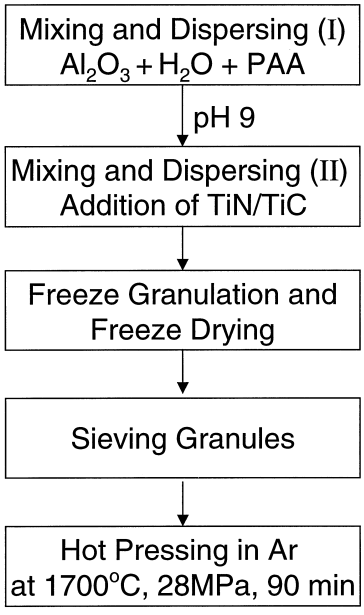

Fig. 3. Processing scheme for composite preparation.

Summarizing the results of our dispersion experiments, we can state that well-dispersed, low-viscous composite suspensions with 20–25 vol.% solids loading (minimum viscosities of the composite suspensions were in the range 3–4 mPa s) can easily be produced with all investigated alumina-based composite systems by using the same processing scheme. An additional advantage of the chosen processing scheme is its tolerance towards variations in degree of surface oxidation of the non-oxide components, which can be difficult to control in industrial practice.

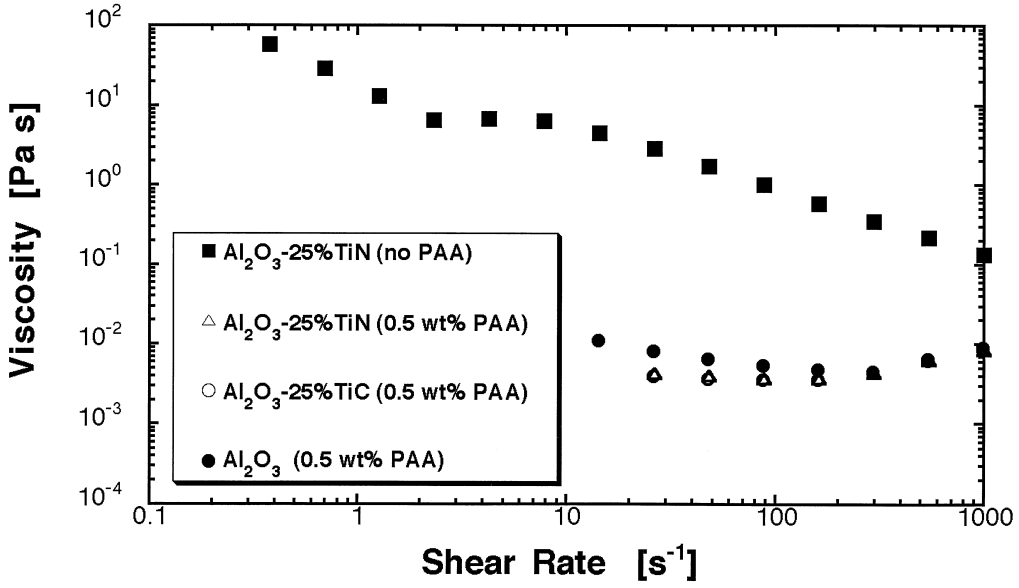

Fig. 4. Steady-shear flow curves of 20 vol.% suspensions at pH≈9.

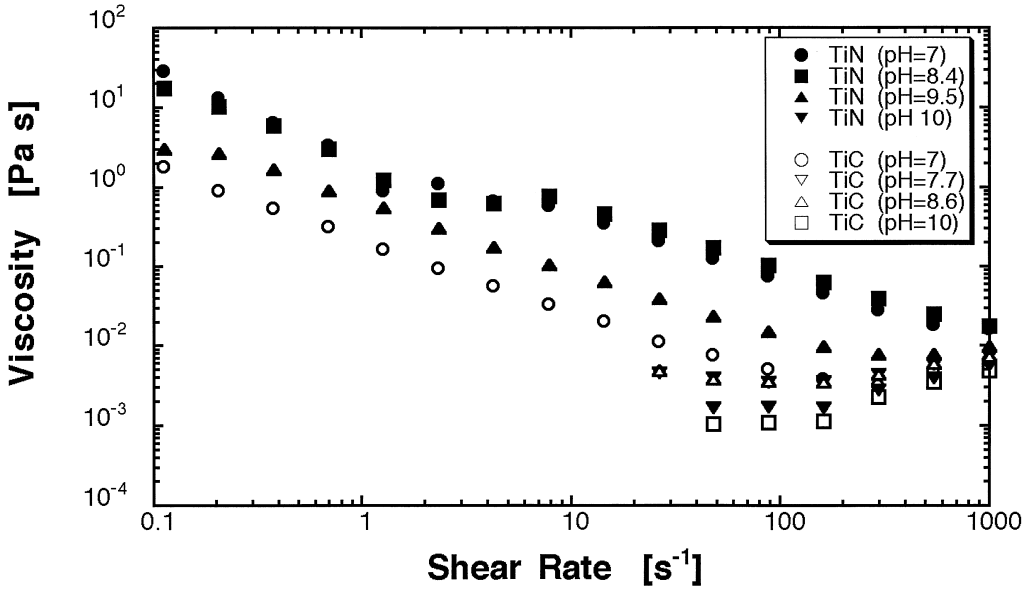

Fig. 5. Steady-shear flow curves of 20 vol.% TiN and TiC suspensions in 0.01 M NaCl electrolyte in the range pH = 7–10.

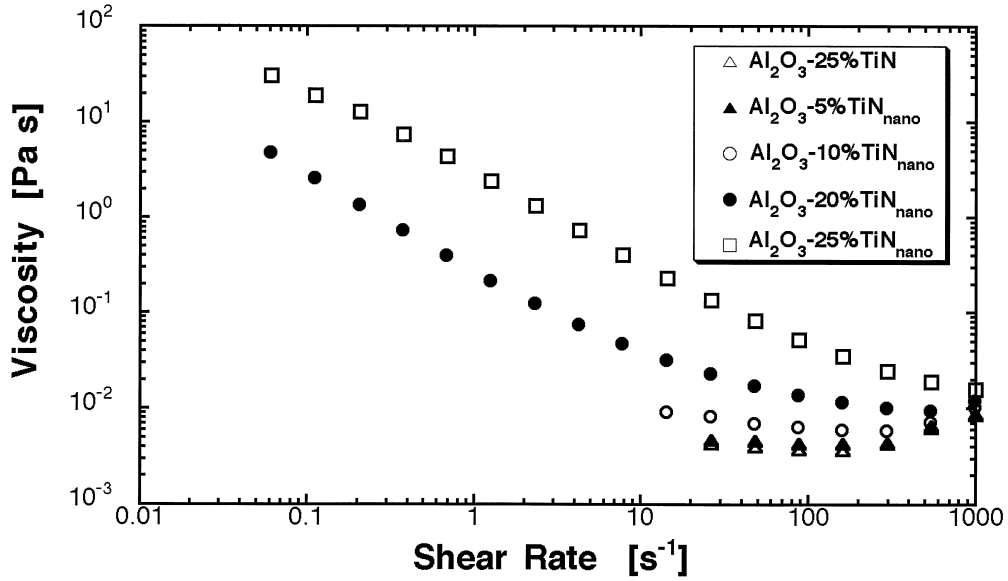

Fig. 6. Steady-shear flow curves of 20 vol.% composite suspensions containing 0.5 wt.% PAA at pH≈9.

3.3. Hot-pressing and microstructure evaluation

From TG studies, it was found that PAA was burned-out completely at 600°C in an Ar–6% H_2 atmosphere. Accordingly, this temperature was chosen to burn out the organic content prior to sintering.

After hot-pressing, the TiC and TiN particle composites were fully densified (Table 3). The amount of PAA added was found to be more critical for microstructure homogeneity of Al_2O_3–TiN composites than for Al_2O_3–TiC composites. Agglomerates of TiN particles could be detected in the microstructure of Al_2O_3–TiN composites. However, their number decreased with increasing PAA concentration and at 0.5 wt.% PAA addition the microstructure was homogeneous with almost no agglomerates (Fig. 7a). This may be related to the effect of pH changes on the colloidal stability of the secondary TiN phase as discussed in the foregoing section; the higher buffer capacity of the suspension at higher PAA concentrations probably reduces the pH change that is induced by addition of the acidic TiN phase. The colloidal stability of the secondary TiC phase is not sensitive to pH changes in the alkaline range as indicated by rheology measurements (Fig. 5). Accordingly,

homogeneous and agglomerate-free microstructures of Al_2O_3–TiC composites were obtained at both 0.25 and 0.5 wt.% PAA content (Fig. 7b).

Composites containing TiC and Ti(C,N) whiskers exhibited high sintered densities, though slightly lower than the particle reinforced composites (Table 3). With an addition of 0.5 wt.% PAA, the resulting microstructure show well-dispersed phases but also traces of porosity (Fig. 8). The whiskers have a preferred orientation perpendicular to the hot-press axis. Obvious defects in the microstructure are due to fibre pull-out during polishing of the samples. XPS measurements indicated a high amount of free carbon on the whisker surfaces. The graphite might weaken the bonding between whisker and alumina matrix, thus facilitating fibre pull-out. Possibly, the hydrophobic graphite also promotes the formation of air bubbles, which are difficult to remove during slurry processing.

Composites containing TiN_{nano} particles were fully densified (Table 3) and exhibited microstructures very much dependent on the added amount of titanium nitride. All nano composites contained micron-sized TiN agglomerates, in amounts increasing with increasing TiN content. In the samples containing 5 vol.% TiN_{nano} the particles and particle agglomerates were well dispersed and homogeneously distributed in the matrix phase. The particles are located both within the alumina grains and at the grain boundaries (Fig. 9a). However, the alumina grain coarsening during sintering was pronounced. At 10 and 20 vol.% TiN_{nano}, the alumina grain coarsening was suppressed; TiN particles formed large agglomerates at the alumina grain boundaries, thus acting as grain growth inhibitors (Fig. 9b and c). Based on these results it is expected that using up to 5 vol.% TiN_{nano} particles in combination with a reduced sintering temperature will result in a microstructure with smaller TiN agglomerates and less excessive alumina grain growth.

Table 3
Compositions of sintered samples and measured density after hot pressing

	Composition	Amount of PAA added with respect to dry powder weight Al_2O_3 (wt.%)	Final density (%ρ_{th})
1	Al_2O_3	0.25	100
2	Al_2O_3	0.5	100
3	Al_2O_3–25 vol.% TiC	0.25	100
4	Al_2O_3–25 vol.% TiC	0.5	100
5	Al_2O_3–25 vol.% TiN	0.25	100
6	Al_2O_3–25 vol.% TiN	0.5	100
7	Al_2O_3–5 vol.% TiN_{nano}	0.5	100
8	Al_2O_3–10 vol.% TiN_{nano}	0.5	100
9	Al_2O_3–20 vol.% TiN_{nano}	0.5	100
10	Al_2O_3–20 vol.% $Ti(C,N)_{whiskers}$	0.5	98
11	Al_2O_3-25 vol.% $TiC_{whiskers}$	0.5	98

4. Summary

The aim of this study has been to develop an aqueous colloidal processing route suitable for Al_2O_3–TiN/TiC

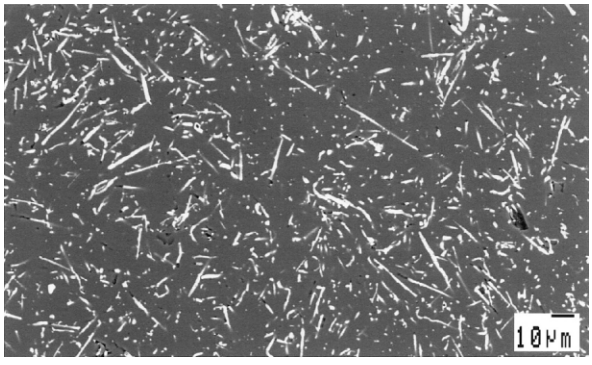

Fig. 8. SEM micrograph of the sample cross-section perpendicular to the pressing direction of hot-pressed Al_2O_3–20 vol.% $Ti(C,N)_{whisker}$ composite (0.5 wt.% PAA).

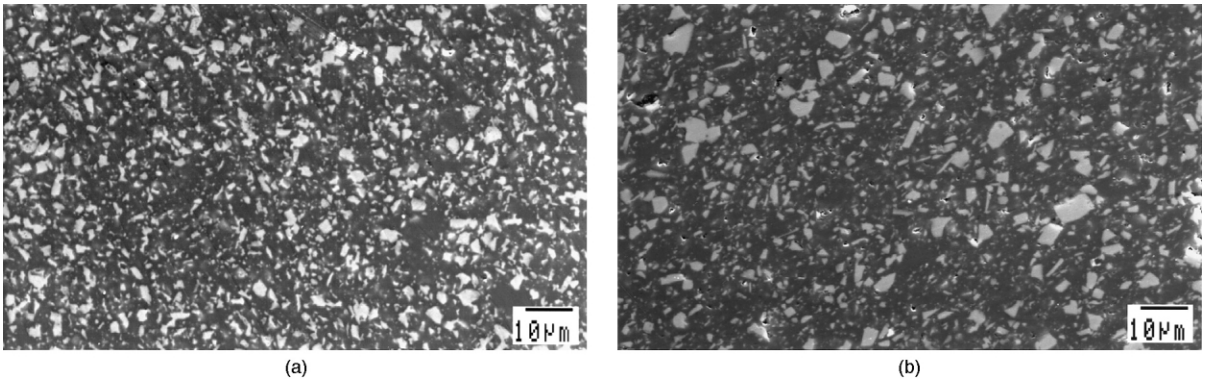

Fig. 7. SEM micrographs of the sample cross-section perpendicular to the pressing direction: (a) Al_2O_3–25 vol.% TiN composite (0.5 wt.% PAA); (b) Al_2O_3–25 vol.% TiC composite (0.5 wt.% PAA).

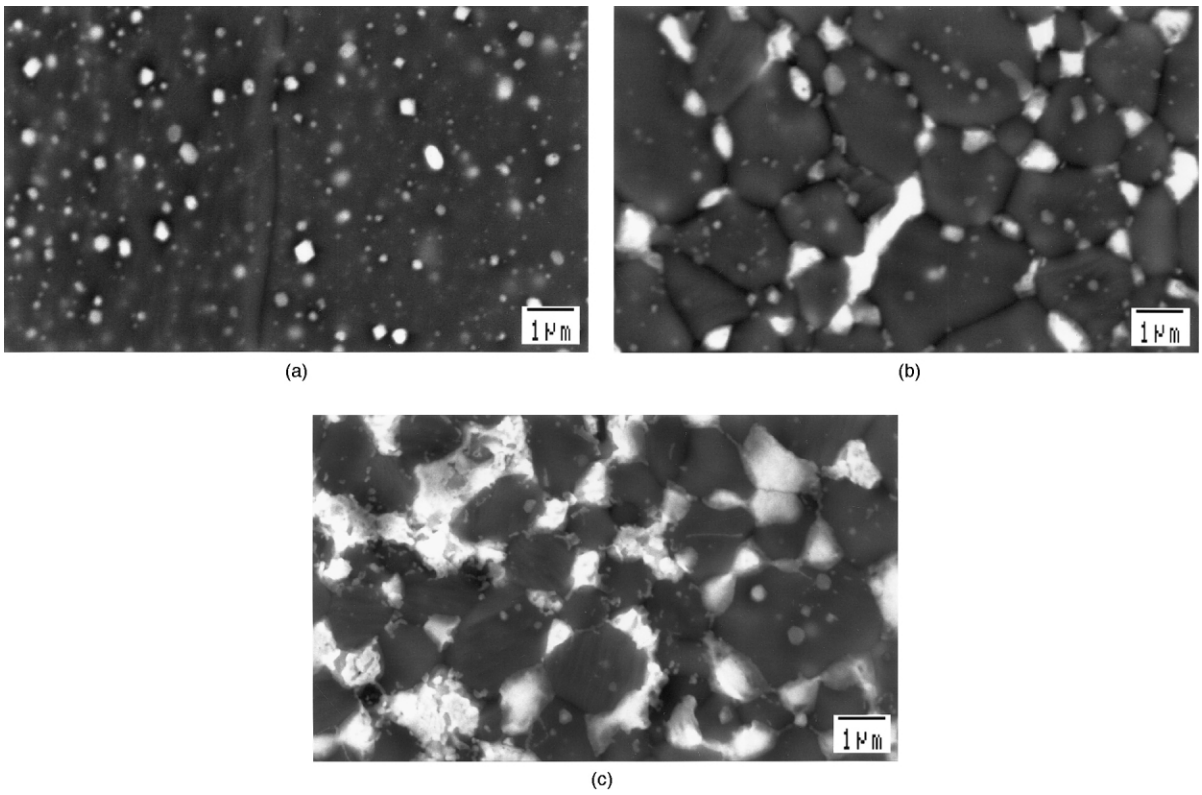

Fig. 9. SEM micrographs of thermally etched cross-sections parallel to the pressure direction of hot-pressed Al_2O_3–TiN_{nano} composites (0.5 wt.% PAA): (a) Al_2O_3–5 vol.% TiN_{nano} (the dark vertical line is a grain boundary between two large alumina grains); (b) Al_2O_3–10 vol.% TiN_{nano}; (c) Al_2O_3–20 vol.% TiN_{nano}.

systems, which can be used for preparation of composites with dense and homogeneous microstructures. Composites containing micron-sized TiN and TiC, nano-sized TiN (~30 nm mean size), TiC whiskers and Ti(C,N) whiskers were investigated. By characterizing the surface chemistry of micron-sized TiN and TiC powders we were able to define appropriate conditions for the wet-processing step. By first dispersing alumina with 0.5 wt.% PAA and then adding the TiN or TiC phase, well-dispersed and colloidally stable composite suspensions with 20 vol.% solids loading could be obtained. The good colloidal stability relates to repulsive electrostatic forces between the alumina particles with adsorbed PAA layers ($pH_{iep} \approx 3$) and the TiN or TiC particles ($pH_{iep} \approx 4.3$) at or above the inherent $pH = 9$ of the suspension. After freeze-granulation of the composite suspension and freeze-drying of the granules, the organic content could be burned out by heating for 15 min at 600°C in a graphite furnace. Sintering was accomplished in a hot-press furnace with flowing argon at 1700°C and 28 MPa for 1.5 h. The assessment of composite microstructures showed that the used processing scheme is applicable to all investigated composite materials. In all cases it is possible to obtain well-dispersed secondary TiN and TiC phases in the alumina matrix phase by controlling suspension pH and added amount PAA. 98–100% of the theoretical density was accomplished after sintering. The homogeneity of TiC containing composite microstructures was not affected by pH variations in the alkaline range during wet processing. For Al_2O_3–TiN composite materials, highly alkaline processing conditions are preferred in order to prevent agglomeration of TiN particulates. Varying the content of TiN_{nano} revealed that there is an optimum concentration below which excessive alumina grain growth occurs whereas at higher concentrations TiN particles tend to form agglomerates at the grain boundaries. The location of the optimum concentration probably depends on the hot pressing conditions. The role of processing parameters in the high-temperature densification step and their influence on mechanical composite properties is the subject of ongoing investigations.

Acknowledgements

This work has been performed within the framework of the Brinell Centre (thematic network "Ceramics and nanocrystalline materials" and "The Brinell Centre-Inorganic Interfacial Engineering"). Financing by the Swedish Foundation for Strategic Research (SSF), the Swedish National Board for Industrial and Technical

Development (NUTEK) and the industrial partners (Erasteel Kloster AB, Ericsson Cables AB, Höganäs AB, Kanthal AB, OFCON Optical Fibre Consultants AB, Sandvik AB, Seco Tools AB, Uniroc AB) is gratefully acknowledged.

References

1. Whitney, E. D. (ed.), *Ceramic cutting tools — materials, development, and performance*. Noyes Publications, Park Ridge, USA, 1994.
2. Johansson, K. E., Palm, T. and Werner, P. E., An automatic microdensitometer for X-ray powder diffraction photographs. *J. Phys. Sci. Instrum.*, 1980, **13**, 1289–1291.
3. Werner, P. E., A fortran program for least-squares refinement of crystal structure cell dimensions. *Arkiv för Kemi*, 1969, **31**, 513–516.
4. Ahlén, N., Johnsson, M. and Nygren, M., Carbothermal synthesis of TiC whiskers via a vapour–liquid–solid growth mechanism. *J. Am. Ceram. Soc.*, 1996, **79**, 2803–2808.
5. Ahlén, N., Johnsson, M. and Nygren, M., Synthesis of TiN_xC_{1-x} whiskers. *J. Mater. Sci. Lett.*, 1999, **18**, 1071–1074.
6. Wagner, J., Janssen, S., Rupp, R., May, R. and Hempelmann, R., Characterization of nanoscale titanium nitride dispersions by small-angle neutron scattering. *J. Am. Ceram. Soc.*, 1998, **81**, 3313–3317.
7. Greenwood, R. and Bergström, L., Electroacoustic and rheological properties of aqueous Ce–ZrO_2 (Ce–TZP) suspensions. *J. Eur. Ceram. Soc.*, 1997, **17**, 537–548.
8. Wäsche, R. and Steinborn, G., Influence of the dispersants in gelcasting of nanosized TiN. *J. Eur. Ceram. Soc.*, 1997, **17**, 421–426.
9. Wäsche, R., Steinborn, G., Baader, F.: Elektrokinetische Messungen zur Charakterisierung wässriger nanodisperser TiN-Suspensionen. *Fortschrittsber. DKG*, 1994, **9**(5), 151–158 (in German).
10. Cesarano III, J. and Aksay, I. A., Processing of highly concentrated aqueous α-alumina suspensions stabilized with polyelectrolytes. *J. Am. Ceram. Soc.*, 1988, **71**, 1062–1067.
11. Bergström, L., Rheological properties of Al_2O_3–SiC whisker composite suspensions. *J. Mater. Sci.*, 1996, **31**, 5257–5270.
12. Santhiya, D., Nandini, G., Subramanian, S., Natarajan, K. A. and Malghan, S. G., Effect of polymer molecular weight on the adsorption of polyacrylic acid at the alumina–water interface. *Colloid Surf. A.*, 1998, **133**, 157–163.
13. Nass, R., Albayrak, S., Aslan, M. and Schmidt, M., Colloidal processing and sintering of nano-scale TiN. In *Ceramic Transactions*, Vol. 51, ed. H. Hausner, G. L. Messing and S.-I. Hirano. American Ceramic Society, Westerville, 1995.
14. Shih, C.-J. and Hon, M.-H., Electrokinetic and rheological properties of aqueous TiN suspensions with ammonium salt of poly(methacrylic acid). *J. Eur. Ceram. Soc.*, 1999, **19**, 2773–2780.
15. Yeh, C.-H. and Hon, M.-H., Dispersion and stabilization of aqueous TiC suspensions. *Ceramics International*, 1995, **21**, 65–68.
16. Bergström, L. and Bostedt, E., Surface chemistry of silicon nitride powders: electrokinetic behaviour and ESCA studies. *Colloids Surf.*, 1990, **49**, 183–197.
17. Zhmud, B. V., Meurk, A. and Bergström, L., Evaluation of surface ionization parameters from AFM data. *J. Colloid Int. Sci.*, 1998, **207**, 332–343.
18. Dupont, L. and Foissy, A., Evaluation of the adsorption trends of a low molecular-weight polyelectrolyte with a site-binding model. *Colloids Surf. A*, 1996, **110**, 235–248.